

Article

Study on the Hydrodynamic Performance of a Countercurrent Total Spray Tray under Sloshing Conditions

Jinliang Tao, Guangwei Zhang, Jiakang Yao, Leiming Wang and Feng Wei *

National-Local Joint Engineering Laboratory for Energy Conservation in Chemical Process Integration and Resources Utilization, School of Chemical Engineering and Technology, Hebei University of Technology, Tianjin 300130, China

* Correspondence: weifeng@hebut.edu.cn; Tel.: +86-135-120-346-32

Abstract: In this paper, a new type of total spray tray (TST) with gas–liquid countercurrent contact is proposed to solve the problem of slight operation flexibility and poor sloshing resistance in towers under offshore conditions. Its hydrodynamic performance indicators, such as pressure drop, weeping, entrainment, and liquid level unevenness, were experimentally studied under rolling motion. A tower with an inner diameter of 400 mm and tray spacing of 350 mm was installed on a sloshing platform to simulate offshore conditions. The experimental results show that the rolling motion affected the hydrodynamic performance of the tray under experimental conditions. When the rolling amplitude did not exceed 4°, the degree of fluctuation of the hydrodynamic performance was small, and the tray could still work stably. With increasing rolling amplitude, the TST wet plate pressure drop, weeping, and liquid level unevenness fluctuations also increased. When the rolling amplitude reached 7°, the maximum fluctuation of the wet plate pressure drop was 8.9% compared to that in the static state, and the plate hole kinetic energy factor, as the TST reached the lower limit of weeping, increased rapidly from 6.2 at rest to 7.8 under the experimental conditions. It can be seen that the TST still exhibits good hydrodynamic performance under rolling motion.

Keywords: pressure drop; countercurrent total spray tray; sloshing platform; hydrodynamic performance; offshore conditions



Citation: Tao, J.; Zhang, G.; Yao, J.; Wang, L.; Wei, F. Study on the Hydrodynamic Performance of a Countercurrent Total Spray Tray under Sloshing Conditions. *Processes* **2023**, *11*, 355. <https://doi.org/10.3390/pr11020355>

Academic Editors: Elio Santacesaria, Riccardo Tesser and Vincenzo Russo

Received: 22 November 2022

Revised: 9 January 2023

Accepted: 19 January 2023

Published: 22 January 2023



Copyright: © 2023 by the authors. Licensee MDPI, Basel, Switzerland. This article is an open access article distributed under the terms and conditions of the Creative Commons Attribution (CC BY) license (<https://creativecommons.org/licenses/by/4.0/>).

1. Introduction

As the most widely used critical common technology in the chemical industry, distillation is widely used in petroleum, natural gas, chemical, pharmaceutical, and environmental protection, and other industries. Furthermore, it occupies a considerable proportion of industrial production [1]. In the 21st century, with the increasing depletion of onshore oil and gas resources and the continuous breakthrough of offshore oil and gas exploration and exploitation technologies, the natural gas industry has begun to extend to the sea [2,3]. The distillation tower is the core equipment of the natural gas pretreatment process, and its operation has a significant impact on the gas purification effect, gas quality, and economic benefits [4]. Therefore, the development of offshore distillation and the realization of stable and efficient distillation towers on offshore platforms have become inevitable trends in the development of the distillation industry [5–9]. However, due to the influence of ocean wind and waves, floating devices will produce three angular motions of rolling, pitching, and yawing, and three displacement motions of swaying, surging, and heaving. The movement of offshore platforms is shown in Figure 1. The sloshing that has the greatest influence on the hydrodynamic performance of a traditional distillation tower is rolling (pitching) [10–12]. Therefore, it is of great significance to understand the performance of the tower under rolling motion.

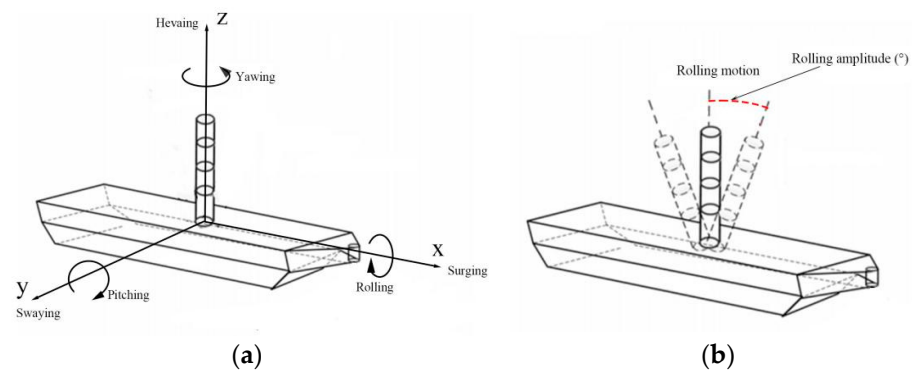


Figure 1. Movement of offshore platform. (a) Movement of offshore platform; (b) rolling motion.

Research on the influence of sloshing on equipment has mainly concentrated on the design calculation and load analysis of ships and tanks [13–16], while research on its effect on towers is relatively rare. Ma [4] carried out an experimental study on bubble cap trays and valve trays on a sloshing platform. The results showed that the performance of the trays decreased significantly with increasing rolling amplitude, and they could not work when the rolling amplitude exceeded 3° . Cheng [17] studied the hydrodynamic performance of LBJ (low backmixing jet) and DLJ (double-layer jet) trays under sloshing conditions and found that their ability to resist sloshing was improved compared to that of traditional trays. Zhang et al. [18] studied the influence of offshore sloshing on a packed column and found that the liquid accumulated obviously near the wall on the tilt side. The flow field parameters in the column changed significantly after the inclination exceeded 3° . Weedman et al. [19] studied the performance of several different packed columns under tilting conditions. Due to the high length–diameter ratio of the distillation column, the separation efficiency decreased rapidly under slight tilting conditions. Di et al. [20] studied the effects of ship motion on the mass transfer area in structured packed columns for offshore gas production. The results confirmed that the mass transfer area will decrease under any typical ship motion. Yang et al. [21] proposed a small air separation plant with a dual-column distillation process and carried out experiments under offshore conditions, providing engineering guidance for the design of cryogenic distillation columns for offshore applications. China University of Petroleum [22–28] conducted an experimental study on a packed column and plate tower on a sloshing platform and analyzed the influence of sloshing on the distribution and flow of gas and liquid in the tower. It was found that rolling motion was the most influential form of sloshing with regard to the hydrodynamic performance of the tower, and the arrangement of partitions could reduce the influence of sloshing on the liquid in the tower.

It can be seen that offshore conditions seriously affect the hydrodynamic performance of packed column and plate towers. The reason for this is that the tilt scale of the tower has a significant amplification effect on the uneven liquid distribution in the tower. For a plate tower with gas–liquid cross-flow contact, the liquid on the tray flows horizontally and cannot be blocked in the flow direction. Thus, the unevenness of liquid on the plate becomes severe with an increasing diameter of the tower under the tilt state. For a packed column with gas–liquid countercurrent contact, the liquid in the column flows vertically downward; by increasing the height of the column, the liquid will deviate to one side of the column during falling into the tilt state. Therefore, the traditional onshore distillation tower cannot maintain high performance under harsh conditions such as sea waves and typhoons [28].

Now, people mainly use different types of packed columns to solve the effect of offshore sloshing on distillation columns. Compared to a packed column, a plate tower has the advantages of a large operating range, suitability for large tower diameters, and convenient maintenance. However, it is impossible to block the liquid in the direction of liquid flow, which limits the application of traditional plate towers in the sea. If the plate tower can be made to resist sloshing, the plate tower will have greater advantages under

some working conditions. Therefore, it is of great significance to study the applicability of plate towers under offshore conditions.

To solve the bottlenecks in existing plate towers—their low operational flexibility and poor resistance to sloshing under sloshing conditions—we propose a new type of total spray tray (TST) [29–31] with gas–liquid countercurrent contact and with the liquid flow in the tower guided by a three-dimensional space barrier. Under rolling conditions, the hydrodynamic performance of this TST was studied experimentally. The variation law of the hydrodynamic performance of the tower plate under offshore conditions is analyzed. Its operational flexibility range is clarified. Its ability to adapt to offshore sloshing conditions is explored, providing technical support for the design optimization of tower equipment on offshore platforms.

2. Materials and Methods

2.1. TST Space Barrier Drainage Principle

The TST consists of three parts: a tray with a plate hole, a spray tube above the plate hole, and a liquid sealing cap. The structure is shown in Figure 2.

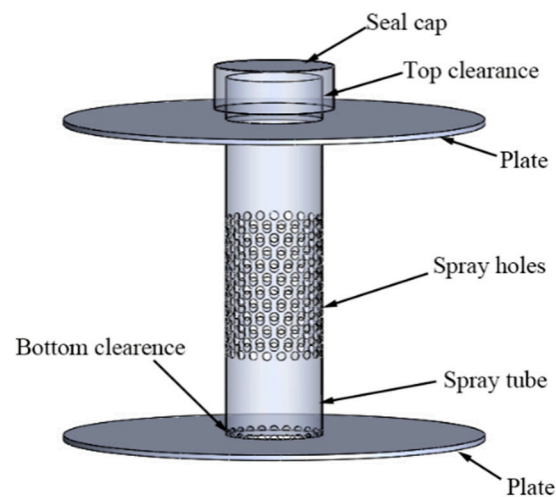


Figure 2. The structure of the TST.

By setting a layer of tray every 350 mm, the liquid will not accumulate obviously near the wall with increasing tower height in the sloshing state. At the same time, because of the gas–liquid countercurrent contact, the liquid does not need to cross the whole tray. The problem with the traditional plate tower where the partitions cannot be increased in the flow direction to reduce the sloshing effect can be solved here by increasing the partitions. The effect of the partitions is shown in Figure 3.

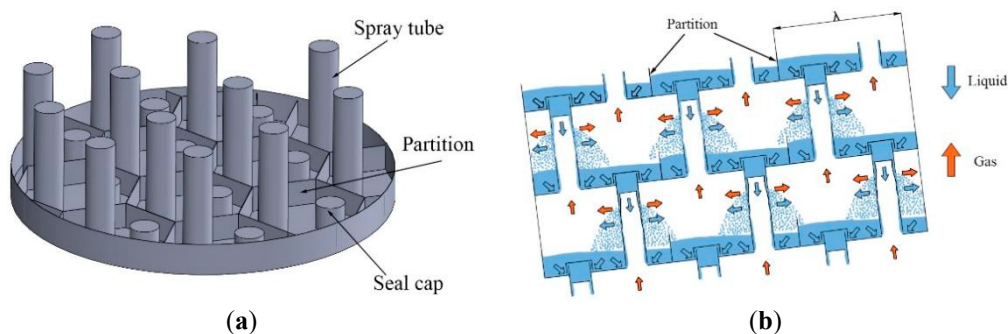


Figure 3. The effect of the partitions. (a) Form of the partitions; (b) working principles of the TST.

2.2. Experimental Setup and Process

The spray tube of the TST has the function of dropping liquid. Thus, the maximum characteristic of the TST is that there is no independent liquid-receiving plate or liquid drop area on the tray, giving the TST the features of structural symmetry in all horizontal directions. Therefore, this paper only studied the influence of the most influential sloshing (rolling) on the hydrodynamic performance of the TST. To simplify the experimental setup, only one barrier unit was analyzed in this experiment, and the diameter of the tower used was 400 mm, that is, $\lambda = 400$ mm. Mobil presented a model wave experiment of the FPSO device in 1998, which showed that under severe sea conditions, the hull roll did not exceed 6° . Han et al. [32] pointed out that the maximum amplitude of rolling or pitching is 5.15° under the once-in-a-century combination of wind and waves along the coast of China. Through the relevant research, it is found that the sloshing period is mostly between 6 s–20 s with regard to the influence of offshore sloshing on the tower. Therefore, combined with experimental conditions, the rolling experiment was carried out at $0\text{--}7^\circ$ and for rolling periods of 8 s, 12 s, 16 s, and 20 s. The gas flow velocity and liquid flow were selected from the normal operating conditions in the static state. The experimental conditions are shown in Table 1.

Table 1. Experimental conditions.

Condition	Value
Liquid flow (m^3/h)	2.2
F_0 ($(\text{m/s})(\text{kg}/\text{m}^3)^{0.5}$)	6–15
F_T ($(\text{m/s})(\text{kg}/\text{m}^3)^{0.5}$)	1.16, 2.01, 2.42
Rolling amplitude ($^\circ$)	0, 1, 2, 3, 4, 5, 6, 7
Rolling period (s)	8, 12, 16, 20

The experimental setup is shown in Figure 4. It consists of a tower, a blower, a circulating pump, a measuring device, and a sloshing platform. The experimental tower used in the experiment was composed of organic glass and PPR (pentatricopeptide repeats) material, with a diameter of 400 mm, a tray spacing of 350 mm, and two fixed TSTs with a diameter of 90 mm. On the spray tube side wall of the TST, 231 holes with a diameter of 8 mm were opened, and 12 half-holes with a diameter of 8 mm were opened on the bottom. The experimental tower was placed on a circulating water tank with a diameter of 600 mm. The highest plate was used to collect entrained liquid. The lowest plate was used to collect weeping liquid. The experimental tower and the circulating water tank were connected to the sloshing platform to slosh together with the sloshing platform. The sloshing platform is shown in Figure 5.

The TST hydrodynamic experiment was carried out under ambient temperature and pressure using an air–water system. During the experiment, gas from an air blower, driven by a frequency conversion motor with 5 kW rated power, was introduced into the bottom of the tower. The velocity of the gas was measured using a pitot tube flowmeter. After the air contacted the liquid phase from bottom to top, it was removed from the vent after passing through the entrainment collector. The water was pumped out by a circulating pump from a circulating water tank and entered from the top of the tower after the rotameter measured the flow. The sloshing platform was controlled by electric machinery to achieve different amplitudes and periods of rolling. The tray pressure drop was measured using a ZCYB-1000 electronic differential pressure gauge, which has an accuracy margin of 1 Pa. After the operation reached stability, the rolling origin was selected as the starting point to start timing, and the pressure drop value was recorded every quarter-period. At the same time, the weeping and entrainment rates were calculated by collecting the weeping liquid and entrained liquid droplets within a certain time in a graduated cylinder. The height of clear liquid could be read from the ruler at the detection point of the tower wall, with an accuracy margin of 1 mm.

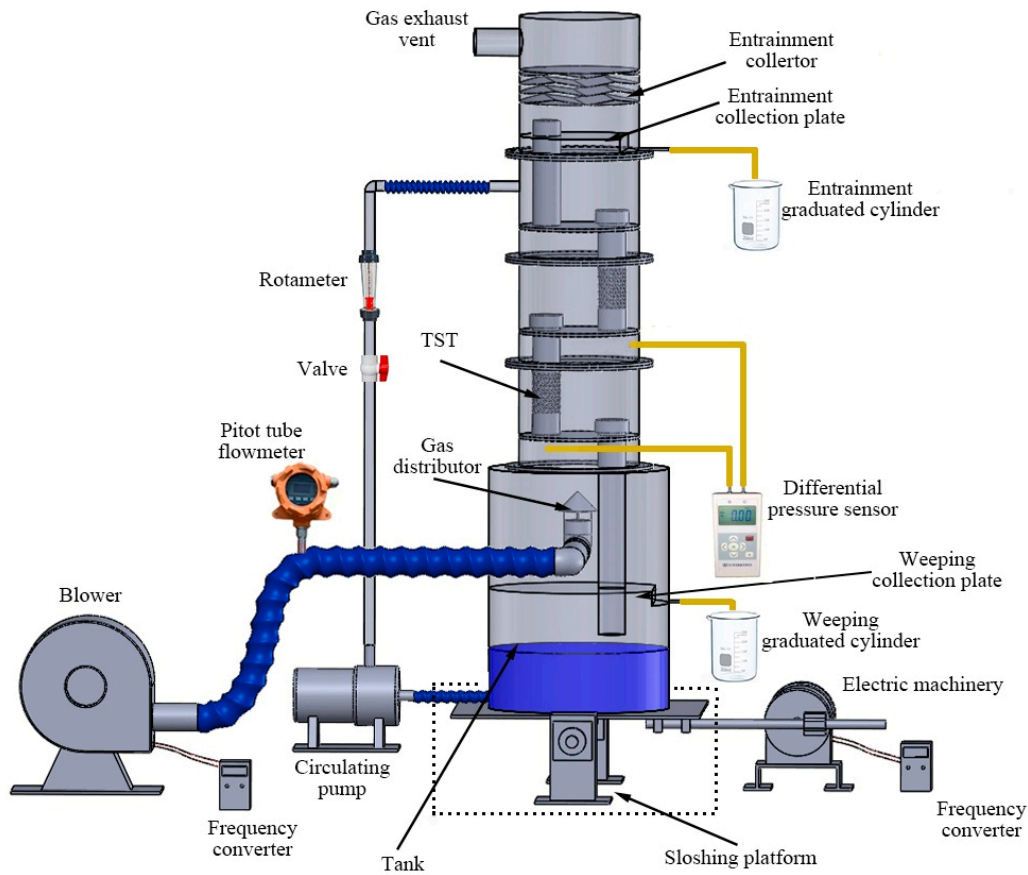


Figure 4. Experimental setup.

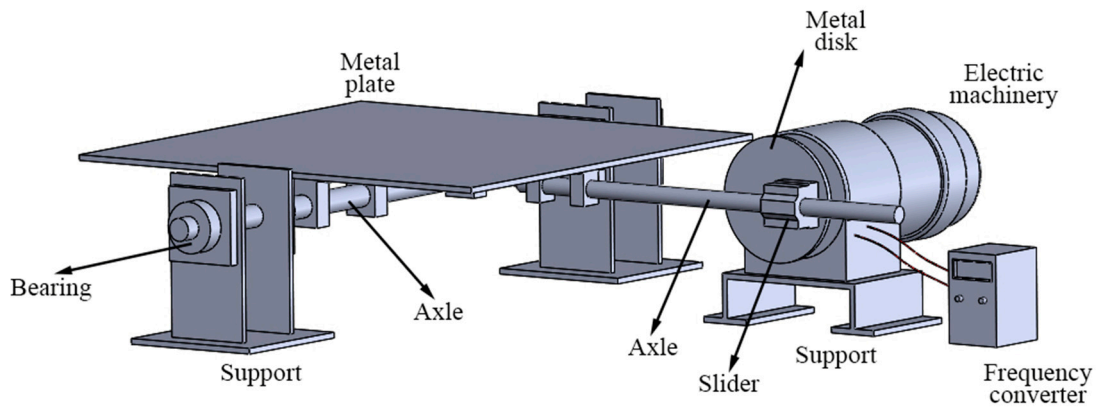


Figure 5. Sloshing platform.

3. Results and Discussion

The offshore rolling motion mainly affects the hydrodynamic performance of the tray. The applicability of the plate tower under offshore conditions is indicated by the hydrodynamic performance of the tray. The following hydrodynamic performance indices are analyzed in this paper.

3.1. Pressure Drop

Plate pressure drop includes dry plate pressure drop and wet plate pressure drop, which are directly related to energy consumption in the operation process. A low pressure drop of the tray means that the fluid flowing through the tray loses less energy. Pressure

drop is an important indicator for evaluating the performance of the tray [33,34]. The pressure drop (ΔP) is calculated via Formula (1):

$$\Delta P = P_b - P_t \quad (1)$$

where P_b is the pressure at the bottom of the tray and P_t is the pressure at the top of the tray.

3.1.1. Dry Plate Pressure Drop

The dry plate pressure drop refers to the energy loss caused by the gas passing through all of the components on the tray when there is no liquid flow, which reflects the influence of the tray structure on the performance [28]. Energy loss in dry pressure drop during TST operation is mainly caused by the gas passing through the plate holes and spray holes.

The change in dry plate pressure drop under different rolling amplitudes of the TST was experimentally analyzed under a rolling period of 8 s and $F_0 = 15$. The experimental results are shown in Figure 6a. At times 0T, 0.5 T, and 1T, the tray was horizontal, and the dry plate pressure drop of the tray was similar to that in the static state. In addition, in a rolling period, the pressure drop at other times was larger than that in the static state. The pressure drop reached the maximum value in the first half-period and the second half-period at 0.25 T and 0.75 T. It can be seen from the figure that when the rolling amplitude was 0–4°, the pressure drop changed little compared to that in the static state, and the maximum pressure drop increased by 20 Pa compared to that in the static state. When the rolling amplitude exceeded 4°, the fluctuation degree of the pressure drop increased significantly. When the rolling amplitude was 7°, the maximum pressure drop increased by 50 Pa. The reason for this is that, due to the influence of rolling, the gas coming out of the plate hole was no longer parallel to the spray tube. This gas directly impacted the inclined spray tube at an angle, making it more likely to form vortices and lose more energy, resulting in an increased pressure drop. With increasing rolling amplitude, the influence is more obvious. It can be seen that rolling had the adverse effect of increasing the TST dry plate pressure drop, but the effect was small when the rolling amplitude was within 4°.

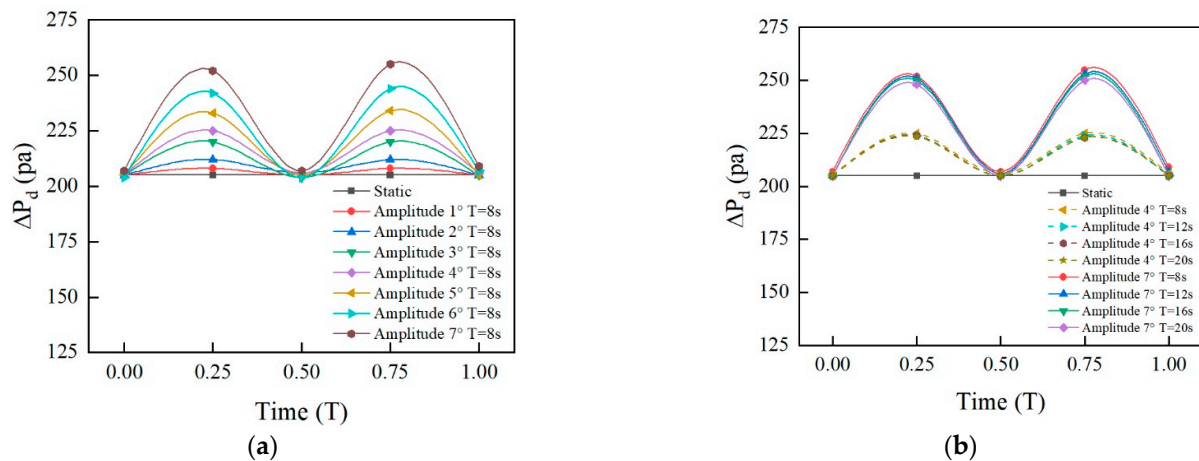


Figure 6. The dry plate pressure drop under rolling motion. (a) Different rolling amplitudes; (b) different rolling periods.

For rolling amplitudes of 4° and 7°, the dry plate pressure drop under different rolling periods was analyzed. The experimental results are shown in Figure 6b. It can be seen that the curve trends of the dry plate pressure drop under different rolling periods were consistent, and the change was small across different rolling periods. When the periods were 8 s and 20 s, the maximum pressure drop difference was only 2%; the pressure drop can thus be considered to be unaffected by the rolling period.

3.1.2. Wet Plate Pressure Drop

The wet plate pressure drop of the TST is different from that of other bubbling trays due to its special structure and gas–liquid flow mode. The wet plate pressure drop of the TST includes two parts: one is the energy loss of gas through the tray structure; the other is the energy lost when the gas contacts the liquid through the spray tube. The wet plate pressure drop of the tray is an important index to evaluate the hydraulic performance of a tower, and it represents the energy lost by the gas phase passing through the tray. According to these data, the tower structure can be improved, which is of great significance to the optimization of the tray structure [35].

Figure 7 shows the change in wet plate pressure drop under rolling motion when $F_0 = 8.74$, $V_L = 2.2 \text{ m}^3/\text{h}$, and $T = 8 \text{ s}$. It can be seen from Figure 7a that when rolling occurred, the pressure drop fluctuated with the rolling and reached maximum fluctuation values in the first half-cycle and the second half-cycle at about $0.25 T$ and $0.75 T$. When the rolling amplitude was not more than 4° , the wet plate pressure drop fluctuated little compared to that in the static state, and when the rolling amplitude reached 4° , the pressure drop at $0.25 T$ and $0.75 T$ changed by 2.3% and 2.7%, respectively, compared to that in the static state. After 4° , the pressure drop fluctuated obviously with increased rolling amplitude. When the rolling amplitude reached 7° , the pressure drops at $0.25 T$ and $0.75 T$ changed by 8.1% and 8.9%, respectively, compared to that in the static state. The reason for this is that the rolling motion causes a fluctuation in the clear liquid layer on the tray, and weeping may occur during this process, which leads to fluctuations in the pressure drop. At $0.25 T$, the spray tube sashes to the lowest position, and the pressure drop increases due to the increase in the liquid level around the spray tube. At $0.75 T$, the spray tube sashes to the highest position and the liquid level at the spray tube is the lowest, resulting in the lowest pressure drop. The larger the rolling amplitude, the greater the pressure drop fluctuation, and the more unstable the working state of the tray.

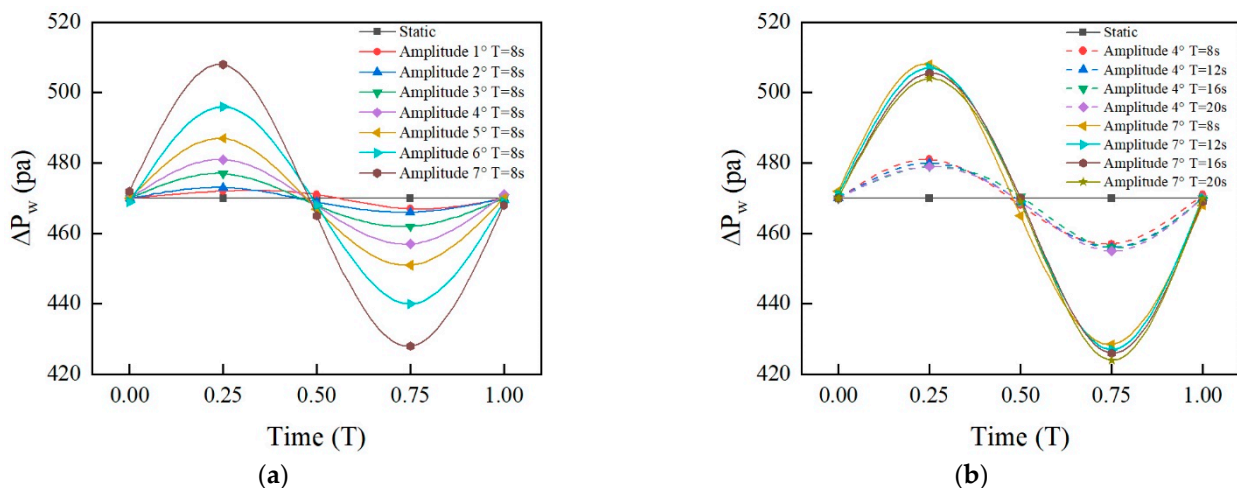


Figure 7. The wet plate pressure drop under rolling motion. (a) Different rolling amplitudes; (b) different rolling periods.

Figure 7b shows that the degree of pressure drop fluctuation under different periods differed little, and the difference between the maximum pressure drop and the minimum pressure drop at $0.25 T$ and $0.75 T$ was only about 1%.

We can see that the wet plate pressure drop under rolling conditions fluctuated with rolling, and the smaller the fluctuation, the stronger the ability to resist sloshing. A rolling amplitude within 4° had little effect on the wet plate pressure drop. When it reached 7° , the fluctuation was controlled at 10%, indicating that the TST can still maintain a good pressure drop distribution under rolling conditions. Further, the change was small under different rolling periods, showing little effect due to the rolling period.

3.2. Weeping

When the rising gas velocity is low, the rising gas' power in the riser is not enough to support the liquid. The liquid directly drops from the riser, which is called weeping. Weeping will affect the plate's gas–liquid contact and reduce the tower plate's efficiency. At the same time, serious weeping will make the plate unable to accumulate fluid, resulting in abnormal operation [29,31]. It is generally considered that the weep rate should not exceed 10%. Therefore, the gas velocity at a weep rate of 10% is called the weep point gas velocity in the industry. The gas velocity at the weeping point is the lower limit of the normal operating range of the tray. The weep rate (e_L) is calculated via Formula (2).

$$e_L = \frac{V_W}{V_L} \quad (2)$$

In the formula, V_W and V_L are the volume flow rates of the weeping liquid and the feed liquid, respectively.

Figure 8 shows the weeping under rolling motion with different F_0 at $V_L = 2.2 \text{ m}^3/\text{h}$. It can be seen from Figure 8a that there was no weeping under the three conditions in the static state, and the weep rate increased with increased rolling amplitude. The growth rate was flat when $F_0 = 8.74$ and $F_0 = 10.05$, and the weep rate was still less than 1% when the rolling amplitude reached 7° . The tray operated well. When $F_0 = 7.86$, the weep rate increased significantly with increased rolling amplitude, and the weep rate reached 7% when the rolling amplitude reached 7° , which is a significant change from the static state. It can be seen that the rolling motion had the adverse effect of increasing the weep rate. At low gas velocity, the rolling motion changes the height of the clear liquid layer and the distribution of the airflow, resulting in the local airflow kinetic energy being insufficient to support the liquid gravity, causing weeping. Moreover, when the rolling amplitude exceeded 4° , the liquid level unevenness increased and the pressure drop fluctuated significantly, so the weep rate increased significantly compared to that from before.

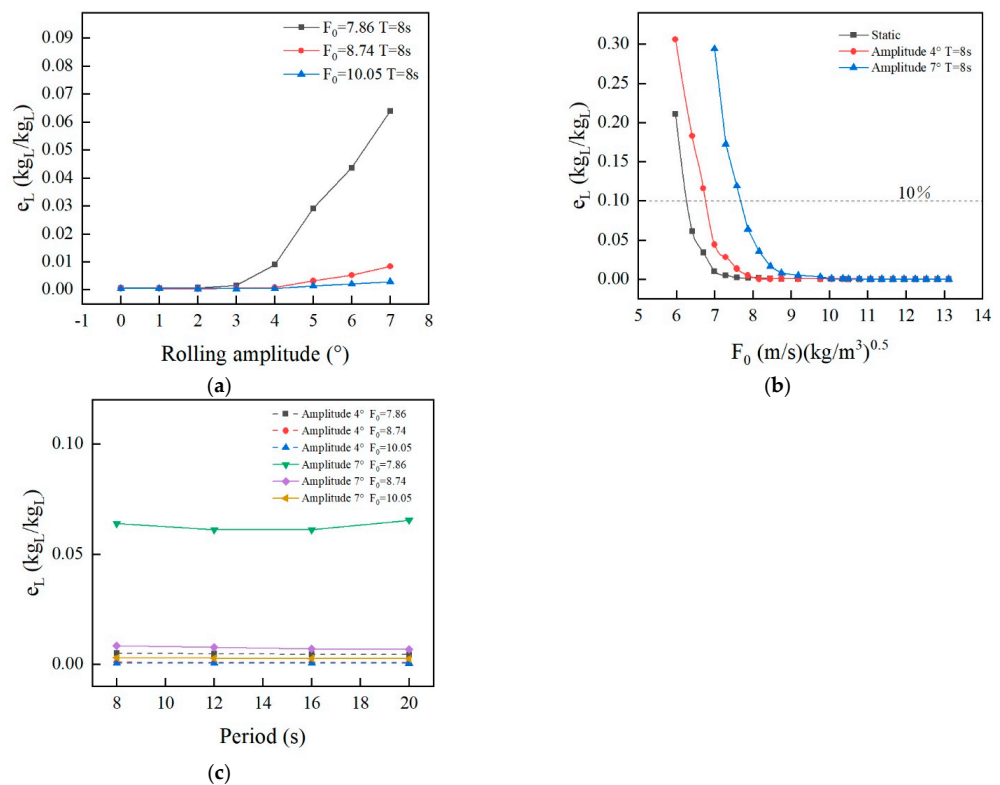


Figure 8. Weeping under rolling motion. (a) Different rolling amplitudes; (b) different gas velocities; and (c) different rolling periods.

It can be seen from Figure 8b that with increased rolling amplitude, the weep rate increased, and the lower operating limit of the tower increased. In the static state, the weep rate reached 10% at $F_0 = 6.3$. When the rolling amplitude was 4° , the weep rate reached 10% at $F_0 = 6.75$. Under a rolling amplitude of 7° , the weep rate reached 10% when $F_0 = 7.7$. We can see that the rolling motion reduced the normal operating range of the tower plate. When the rolling amplitude was 4° , the lower operating limit of the tower increased by about 7.5% compared to that in the static state, having little effect on the tower. When the rolling amplitude was 7° , the lower operating limit of the tower increased by about 22% compared to that in the static state. However, the weep rate can still be well controlled under the appropriate plate hole kinetic energy factor. Figure 8c shows that as the rolling period changed in the range of 8 s ~ 20 s, the differences between the weep rates of each period were small and could be ignored.

3.3. Entrainment

When the gas flow velocity is low, weeping occurs, making the tray unable to operate normally. Conversely, when the gas velocity is too large, some small droplets will be carried by the gas to the upper tray, which is called entrainment. Excessive entrainment will affect the efficiency of the tower [36]. In industrial production, remedial measures must be taken when entrainment reaches 5% [37]. Entrainment is calculated via Formula (3):

$$e_v = \frac{M_e}{M_G} \quad (3)$$

where M_e is the mass rate of the liquid lifted to the foam capture tray by the gas and M_G is the mass rate of the gas.

In order to better study the entrainment of the tray, experimental analysis was carried out with different F_T at $V_L = 2.2 \text{ m}^3/\text{h}$. It can be seen from Figure 9a that with increasing rolling amplitude, the entrainment tended to decrease, and the larger the gas velocity, the more obvious the change trend. When $F_T = 1.16$, the tray had no entrainment under the rolling condition as it was under the static state, and when $F_T = 2.42$, the entrainment decreased slightly with increased rolling amplitude.

It can be seen from Figure 9b that the entrainment was positively correlated with F_T and decreased with increased rolling amplitude. When $F_T = 2.42$, the entrainment was reduced by about 5% compared to that in the static state when the rolling amplitude was 4° , and it was reduced by 9% when the rolling amplitude was 7° . The reason for this is that, due to the influence of rolling, in the process of gas-liquid injection, part of the gas is sprayed downward and part of the gas is sprayed upward. The gas and liquid sprayed obliquely downward will directly fall on the tray, and due to the effect of gravity, the liquid-carrying rate of this part of the gas is relatively higher. Rolling increases the collision between the droplets and the tower components so that some of the small droplets converge into large droplets after collision and fall directly. The higher the gas velocity, the greater the collision's severity. Therefore, rolling causes the entrainment to slightly decrease.

Figure 9c shows that when F_T was low, the rolling period did not affect the entrainment. When F_T was high, entrainment increased with increased period length. When the rolling amplitudes were 4° and 7° under the condition of $F_T = 2.42$, the entrainment ratios in the 20 s period increased by 4.1% and 5.3%, respectively, compared to that in the 8 s period. The reason for this is that, with an increase in the rolling period length, the collision intensity between droplets decreases, which makes the entrainment rise.

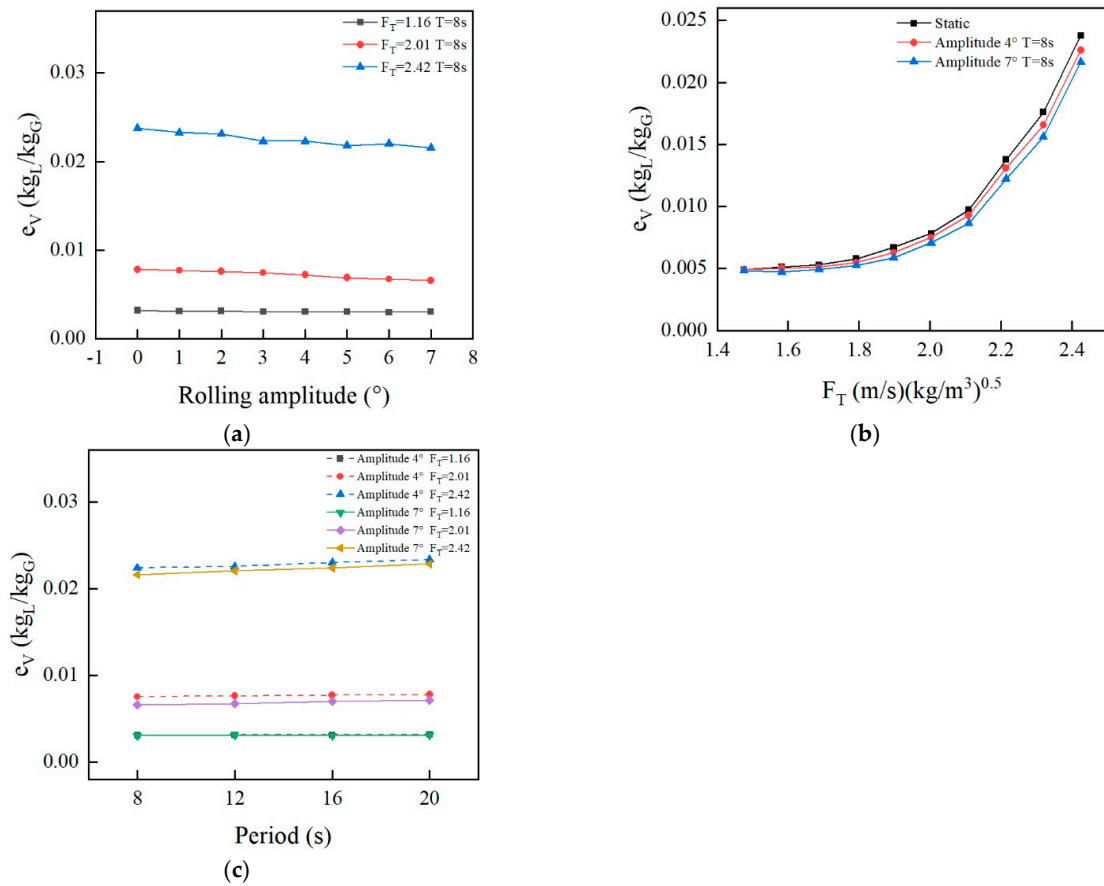


Figure 9. Entrainment under rolling motion. (a) Different rolling amplitudes; (b) different gas velocities; and (c) different rolling periods.

3.4. Liquid Level Unevenness

When the tower is tilted due to rolling motion, the free liquid level on the plate will be different, and the liquid level at each position will change at any time with the rolling. In this paper, the degree of liquid level unevenness at a certain time is called the liquid level unevenness. The greater the liquid level unevenness is, the greater the pressure drop fluctuation of the tray is, and the easier it is to cause weeping and other adverse effects. Eight test points were taken on the tower wall in the experiment, as shown in Figure 10.

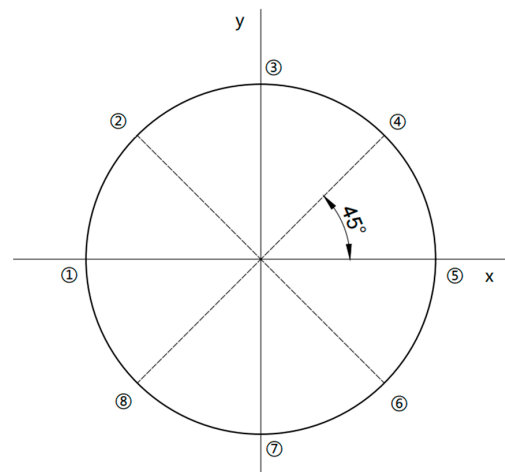


Figure 10. The locations of monitoring points.

In this experiment, the diameter of the tower and the frequency of rolling were small, so it can be considered that the free liquid level on the tower plate was still in the horizontal state and did not fluctuate during the rolling. The liquid layer on the tray had a clear free liquid level, which could be read directly. We reduced the observation error by measuring the liquid level under multiple periods and calculating the average value. After measuring the liquid level at the eight points, the liquid level unevenness was calculated according to Formula (4).

$$M_f = \left[\frac{1}{n} \sum_{i=1}^n \left(\frac{h_i - \bar{h}}{\bar{h}} \right)^2 \right]^{0.5} \quad (4)$$

In the formula, n represents the number of measuring points on the tower wall; h_i represents the liquid level at point i on the tower wall, mm; and \bar{h} represents the average liquid level height on the tray, mm.

Figure 11 shows the influence of different rolling amplitudes and rolling periods on the liquid level unevenness when $F_0 = 8.74$ and $V_L = 2.2\text{m}^3/\text{h}$. Figure 11a shows that the liquid level unevenness under different rolling amplitudes fluctuated periodically with time, reaching upper and lower half-period maxima at around $0.25 T$ and $0.75 T$. The fluctuation in amplitude of liquid level unevenness increased with increased rolling amplitude. Figure 11b shows that the trend of level unevenness on the tower plate was consistent under different rolling periods, and the difference between each period was small enough to be ignored. It can be seen that rolling motion had adverse effects on free surface fluctuation, but there was no sharp change in the free surface in the experiment, and the tray could still work normally.

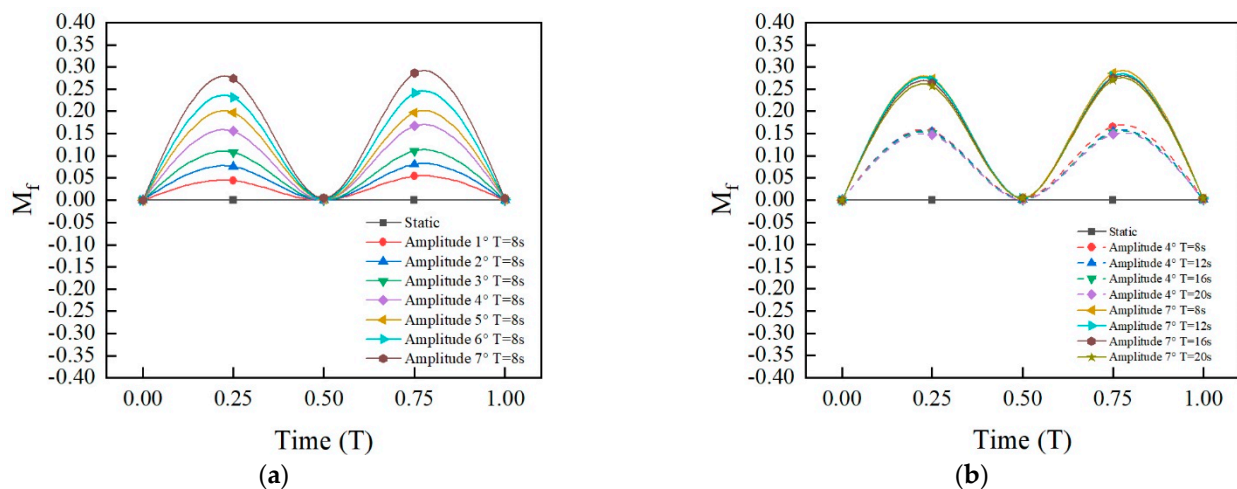


Figure 11. Liquid level unevenness under rolling motion. (a) Different rolling amplitudes; (b) different rolling periods.

4. Conclusions

In this paper, a new type of total spray tray (TST) with gas–liquid countercurrent contact was proposed to solve the problem of poor resist sloshing ability in existing towers under offshore conditions. Its hydrodynamic performance was experimentally studied under rolling motion to evaluate the influence of offshore conditions on the TST. The following conclusions were obtained under the experimental conditions:

Rolling caused adverse effects such as hydrodynamic performance fluctuation of the tray. When the rolling amplitude did not exceed 4° , the fluctuation was small. As the rolling amplitude exceeded 4° , the influence of rolling on the TST gradually increased.

The dry plate pressure drop of the TST fluctuated with the rolling motion. When the rolling amplitude was 4° , the dry plate pressure drop fluctuated by a maximum of 9% compared to that in the static state, and the fluctuation was 22% when the rolling amplitude

was 7°. The fluctuation amplitude of wet plate pressure drop increased with increased rolling amplitude. When the rolling amplitude was 4°, the maximum fluctuation of wet plate pressure drop was 2.7% compared to that in the static state, and when the rolling amplitude was 7°, the fluctuation was 8.9%.

Rolling induced weeping, reducing the normal range of the tray. When the rolling amplitude was 4°, the lower limit of operation of the tray was 7.5% higher than that in the static state, which had little effect on the tower. At 7°, the lower limit of operation of the tray was 22% higher than that in the static state. However, under the condition of an appropriate kinetic energy factor, the weep rate could still be well controlled within 10%.

Entrainment decreased slightly with an increase in the rolling amplitude, which shows that the rolling motion had little effect on the entrainment. The fluctuation in liquid level unevenness increased with increased rolling amplitude. However, there was no serious liquid level fluctuation at large amplitudes, and the tower could still operate stably.

The difference in the hydrodynamic performance of the TST in different periods was very small, so different rolling periods can be considered to have little effect on the performance of the tray.

At the same time, it can be seen that increasing the gas velocity within the appropriate range can reduce the adverse effects such as weeping caused by sloshing in practical applications.

Author Contributions: Conceptualization, methodology, J.T.; data curation, writing—original draft, software, G.Z.; validation, J.Y.; software, L.W.; writing—review and editing, F.W. All authors have read and agreed to the published version of the manuscript.

Funding: This research received no external funding.

Institutional Review Board Statement: Not applicable.

Informed Consent Statement: Not applicable.

Data Availability Statement: Not applicable.

Conflicts of Interest: The authors declare no conflict of interest.

Nomenclature

e_L	$e_L = \frac{V_w}{V_L}$ relative weeping
e_v	$e_v = \frac{L_2 \rho_L}{M_v}$ gas entrainment
F_0	$F_0 = u_0 \sqrt{\rho_G}$ plate hole kinetic energy factor ((m/s)(kg/m ³) ^{0.5})
F_T	$F_T = u_T \sqrt{\rho_G}$ empty tower kinetic energy factor ((m/s)(kg/m ³) ^{0.5})
h_i	liquid level at point i on the tower wall (mm)
\bar{h}	average liquid level on the tray (mm)
L_w	volume of liquid per unit time (m ³ /h)
M_e	mass rate of the liquid (kg/h)
M_f	unevenness of liquid level
M_G	mass rate of the gas (kg/h)
n	number of measuring points on the tower wall
ΔP	pressure drop (Pa)
P_d	pressure at the bottom of the tray (Pa)
P_t	pressure at the top of the tray (Pa)
ΔP_d	dry pressure drop across the tray (Pa)
ΔP_w	wet pressure drop across the tray (Pa)
u_0	velocity of the gas in the plate holes (m/s)
u_T	velocity of the gas in the empty column (m/s)
T	period (s)
V_L	volume flow rates of the weeping liquid (m ³ /h)
V_w	volume flow rates of the feed liquid (m ³ /h)

Greek symbols

θ	deviation angle of the column axis from the vertical axis (°)
ρ_G	density of the gas (kg/m ³)
ρ_L	density of the liquid (kg/m ³)
λ	partition spacing (mm)

References

- Hailun, R.; Dengchao, A.; Taoyue, Z.; Hailong, L.; Xingang, L. Distillation technology research progress and industrial application. *Chem. Ind. And. Eng. Prog.* **2016**, *35*, 1606–1626.
- Chengzao, J.; Yongfeng, Z.; Xia, Z. Prospects of and challenges to natural gas industry development in China. *Nat. Gas Ind.* **2014**, *34*, 8–18. [[CrossRef](#)]
- Wenhua, Z. Numerical and Experimental Study on Hydrodynamics of an FLNG System. Ph.D. Thesis, Shanghai Jiao Tong University, Shanghai, China, 2014.
- Ma, P. Studies on Adaptation of Plate Column in FLNG Unit. Master's Thesis, China University of Petroleum (EastChina), Dongying, China, 2017.
- Jiwei, S. Key Technology Research in FLNG General Design. *Shipbuild. China* **2015**, *56*, 81–86.
- Bin, X.; Xichong, Y.; Xuliang, H.; Yan, L. Research status of FLNG and its application prospect for deep water gas field development in South China Sea. *China Offshore Oil Gas* **2017**, *29*, 127–134.
- Bin, X.; Shisheng, W.; Xichong, Y.; Xia, H. FLNG/FLPG engineering models and their economy evaluation. *Nat. Gas Ind.* **2012**, *32*, 99–102+119–120.
- Scott, E.B.; Lane, M.K. SS: Floating Offshore LNG: Offshore LNG Value Chain Optimization. In Proceedings of the Offshore Technology Conference, Houston, TX, USA, 4–7 May 2009.
- Wijngaarden, W.V.; Meek, H.J.; Schier, M. The Generic LNG FPSO—A Quick & Cost-Effective Way to Monetize Stranded Gas Fields. In Proceedings of the SPE Asia Pacific Oil and Gas Conference and Exhibition, Perth, Australia, 20–22 October 2008.
- Gu, Y.; Ju, Y. LNG-FPSO: Offshore LNG solution. *Front. Energy Power Eng. China* **2008**, *2*, 249–255. [[CrossRef](#)]
- Chun, Z. Studies on Floating LNG Pretreatment Technology of Liwan Gas Field in the South China Sea. Master's Thesis, China University of Petroleum, Dongying, China, 2011.
- Jianfeng, T.; Qiang, C.; Haojie, Z.; Wengang, Y.; Qingyan, X.; Zelin, S. Effect of shaking on pressure drop of structured packing absorption column. *J. China Univ. Pet. Ed. Nat. Sci.* **2018**, *42*, 142–148.
- Hafez, K.; El-Kot, A.-R. Comparative analysis of the separation variation influence on the hydrodynamic performance of a high speed trimaran. *J. Mar. Sci. Appl.* **2011**, *10*, 377–393. [[CrossRef](#)]
- Piller, M.; Nobile, E.; Hanratty, T.J. DNS study of turbulent transport at low Prandtl numbers in a channel flow. *J. Fluid Mech.* **2002**, *458*, 419–441. [[CrossRef](#)]
- Chengsheng, W.; Decai, Z.; Bo, L.; Lei, G. CFD Computation of Ship Motions and Added Resistance for a High Speed Trimaran in Regular Heading Waves. *Shipbuild. China* **2010**, *51*, 1–10.
- Shuxi, T. Sloshing Load Analysis for FLNG Tank Design. Master's Thesis, Dalian University of Technology, Dalian, China, 2012.
- Cheng, Q. Study on Performance Evaluation of Two New Types of Tray on FLNG. Master's Thesis, China University of Petroleum (EastChina), Dongying, China, 2018.
- Zhang, M.; Li, Y.; Li, Y.; Han, H.; Teng, L. Numerical simulations on the effect of sloshing on liquid flow maldistribution of randomly packed column. *Appl. Therm. Eng.* **2017**, *112*, 585–594. [[CrossRef](#)]
- Weedman, J.A.; Dodge, B.F. Rectification of Liquid Air in a Packed Column. *Ind. Eng. Chem.* **2002**, *39*, 732–744. [[CrossRef](#)]
- Di, X.; Ma, J.; Huang, Y. Mass-transfer area in a pilot-scale structured-packing column under different types of ship motion. *Chem. Eng. Sci.* **2019**, *203*, 302–311. [[CrossRef](#)]
- Meng, Y.; Wang, S.; Zhang, Y.; Chen, S.; Hou, Y.; Chen, L. Experimental evaluation of the performance of a cryogenic distillation system under offshore conditions. *Chem. Eng. Sci.* **2022**, *263*, 118084. [[CrossRef](#)]
- Bin, H. Studies on Decarbonisation Performance of Packed Absorption Tower under Sloshing Conditions. Master's Thesis, China University of Petroleum (EastChina), Dongying, China, 2016.
- Fan, Y. Studies on Distributing Performance of ladder liquid distributor Under Sloshing Conditions. Master's Thesis, China University of Petroleum (EastChina), Dongying, China, 2016.
- Zelin, S. Studies on Flow Performance of Structured Packing in Absorption Tower under the shaking Condition. Master's Thesis, China University of Petroleum (EastChina), Dongying, China, 2016.
- Kai, Z. Studies on Decarbonization Tower Design Optimization Under Sloshing Conditions. Master's Thesis, China University of Petroleum (EastChina), Dongying, China, 2015.
- Jianfeng, T.; Jian, C.; Yunfei, X.; Wengang, Y.; Xinpeng, J.; Weiming, Z. Research on orifices diameter of calandria liquid distributor used in offshore deacidification tower with different spray densities. *Chem. Ind. Eng. Prog.* **2017**, *36*, 1192–1201.
- Jianfeng, T.; Xinming, J.; Junyi, Z.; Wengang, Y.; Jian, C.; Haojie, Z. Compatibility test of gas distributor in the FLNG packed tower. *Oil Gas Storage Transp.* **2018**, *37*, 822–830.
- Jianfeng, T.; Bin, H.; Xinming, J.; Yihuai, H.; Zelin, S.; Qiang, C. Fluid distribution performance of packed tower under coupling sloshingworking conditions. *J. China Univ. Pet. Ed. Nat. Sci.* **2017**, *41*, 130–137.

29. Yanli, L.; Jinliang, T.; Bo, L.; Zhicheng, S.; Feng, W. Study on hydrodynamics performance and mass transfer efficiency of total spray tray. *Mod. Chem. Ind.* **2018**, *38*, 200–204.
30. Tao, J.L.; Shi, Z.C.; Ling, Y.L.; Wei, F. Hydrodynamic Characteristics in the Counter-Flow Total Spray Tray. *Chem. Eng. Technol.* **2019**, *42*, 1199–1204. [[CrossRef](#)]
31. Ran, W.; Jinliang, T.; Yanli, L.; Feng, W.; Jidong, L. Total spray tray (TST) for distillation columns: A new generation tray with lower pressure drop. *Chem. Ind. Chem. Eng. Q.* **2017**, *23*, 523–527. [[CrossRef](#)]
32. Xuliang, H.; Bin, X.; Xiaosong, Z.; Jingrui, Z. Numerical Simulation and Experimental Study on Hydrodynamic Performance of FLNG with Liquid Tanks. *Shipbuild. China* **2016**, *57*, 87–97.
33. Wang, H.; Niu, X.; Li, C.; Li, B.; Yu, W. Combined trapezoid spray tray (CTST)—A novel tray with high separation efficiency and operation flexibility. *Chem. Eng. Process.* **2017**, *112*, 38–46. [[CrossRef](#)]
34. Tang, M.; Zhang, S.; Wang, D.; Liu, Y.; Zhang, Y.; Wang, H.; Yang, K. Hydrodynamics of the tridimensional rotational flow sieve tray in a countercurrent gas-liquid column. *Chem. Eng. Process.* **2019**, *142*, 107568. [[CrossRef](#)]
35. Zhang, M.; Zhang, B.Y.; Zhao, H.K.; Zhao, Y.; Sun, J.; Ren, Z.Q.; Li, Q.S. Hydrodynamics and mass transfer performance of flow-guided jet packing tray. *Chem. Eng. Process.* **2017**, *120*, 330–336. [[CrossRef](#)]
36. Jaćimović, B.M. Entrainment effect on tray efficiency. *Chem. Eng. Sci.* **2000**, *55*, 3941–3949. [[CrossRef](#)]
37. Kister, H.Z.; Haas, J.R. Entrainment from sieve trays in the froth regime. *Ind. Eng. Chem. Res.* **2002**, *27*, 2331–2341. [[CrossRef](#)]

Disclaimer/Publisher’s Note: The statements, opinions and data contained in all publications are solely those of the individual author(s) and contributor(s) and not of MDPI and/or the editor(s). MDPI and/or the editor(s) disclaim responsibility for any injury to people or property resulting from any ideas, methods, instructions or products referred to in the content.